Long-range Ca2+ waves transmit brain-damage signals to microglia

Sieger, Dirk ; Moritz, Christian ; Ziegenhals, Thomas ; Prykhozhij, Sergey ; Peri, Francesca

Abstract: Microglia are the resident phagocytes of the brain that are responsible for the clearance of injured neurons, an essential step in subsequent tissue regeneration. How death signals are controlled both in space and time to attract these cells toward the site of injury is a topic of great interest. To this aim, we have used the optically transparent zebrafish larval brain and identified rapidly propagating Ca2+ waves that determine the range of microglial responses to neuronal cell death. We show that while Ca2+-mediated microglial responses require ATP, the spreading of intercellular Ca2+ waves is ATP independent. Finally, we identify glutamate as a potent inducer of Ca2+-transmitted microglial attraction. Thus, this real-time analysis reveals the existence of a mechanism controlling microglial targeted migration to neuronal injuries that is initiated by glutamate and proceeds across the brain in the form of a Ca2+ wave.

DOI: https://doi.org/10.1016/j.devcel.2012.04.012

Originally published at:
Sieger, Dirk; Moritz, Christian; Ziegenhals, Thomas; Prykhozhij, Sergey; Peri, Francesca (2012). Long-range Ca2+ waves transmit brain-damage signals to microglia. Developmental Cell, 22(6):1138-1148.
DOI: https://doi.org/10.1016/j.devcel.2012.04.012

Developmental Cell
Article

Long-Range Ca^{2+} Waves Transmit Brain-Damage Signals to Microglia

Dirk Sieger,[1,3] Christian Moritz,[1,3] Thomas Ziegenhals,[1] Sergey Prykhozhij,[2] and Francesca Peri[1,*]
[1]EMBL Heidelberg, Meyerhofstraße 1, 69117 Heidelberg, Germany
[2]MPI for Molecular Genetics, Ihnestraße 63-73, 14195 Berlin, Germany
[3]These authors contributed equally to this work
*Correspondence: peri@embl.de
DOI 10.1016/j.devcel.2012.04.012

SUMMARY

Microglia are the resident phagocytes of the brain that are responsible for the clearance of injured neurons, an essential step in subsequent tissue regeneration. How death signals are controlled both in space and time to attract these cells toward the site of injury is a topic of great interest. To this aim, we have used the optically transparent zebrafish larval brain and identified rapidly propagating Ca^{2+} waves that determine the range of microglial responses to neuronal cell death. We show that while Ca^{2+}-mediated microglial responses require ATP, the spreading of intercellular Ca^{2+} waves is ATP independent. Finally, we identify glutamate as a potent inducer of Ca^{2+}-transmitted microglial attraction. Thus, this real-time analysis reveals the existence of a mechanism controlling microglial targeted migration to neuronal injuries that is initiated by glutamate and proceeds across the brain in the form of a Ca^{2+} wave.

INTRODUCTION

Positional information in the shape of diffusible signals is often used to guide motile cells toward specific targets. An excellent model to address this basic question is provided by the long-range targeting of migrating leukocytes to the site of induced injury (Wood and Jacinto, 2007; Niethammer et al., 2009; Moreira et al., 2010). Recent work has shown that the attraction of zebrafish leukocytes to wounds in the caudal fin involves an H_2O_2 gradient (Niethammer et al., 2009). In addition to these freely moving leukocytes, there are defined subsets of phagocytes that are known to take up residence in specific organs. The most intensively studied among these are the microglia of the brain, whose function is to clear the brain of dying neurons (Hanisch and Kettenmann, 2007; Napoli and Neumann, 2009; Neumann et al., 2009; Ransohoff and Cardona, 2010; David and Kroner, 2011; Schlegelmilch et al., 2011). It has recently been suggested that, in addition to this key role, these cells might be involved in controlling behavior via synaptic pruning (Chen et al., 2010; Paolicelli et al., 2011). Therefore, it is not surprising that the positioning of microglia and their targeting toward neurons is a topic of great interest. One key signal is ATP, which is detected by P2Y12 receptors that are expressed by microglia (Haynes et al., 2006). Perturbing ATP distribution, either by injection of apyrase, an ATP-hydrolyzing enzyme, or saturation by injection of ATP into the brain, blocks the response of microglia to neuronal injury (Davalos et al., 2005). While a requirement for extracellular ATP in the attraction of microglia is clear, the mechanism by which this signal propagates is controversial. The simplest model suggests that diffusion of ATP from the injury sites generates a gradient that guides microglia directly. However, as extracellular ATP is rapidly degraded by ectonucleotidases, such an attractant gradient is likely to be limited in range (Zimmermann, 2000). An alternative relay model suggests that ATP at the injury site triggers subsequent ATP release by cells along the path; however, the signals that mediate such a relay await identification. Interestingly, it has been shown that bulk exocytosis of ATP-containing vesicles is often dependent on cytosolic Ca^{2+} levels, suggesting a possible link between Ca^{2+} signaling and microglial attraction via ATP (Pangrsic et al., 2007; Striedinger et al., 2007; Liu et al., 2011). One important advance in our understanding of microglial targeting to injury sites would be the development of tools that allow the visualization of death signaling as it propagates across the brain. Here, we have developed transgenic lines in zebrafish to study these processes in the living brain. By performing targeted laser neuronal ablations in the brains of transgenic calcium reporter fish, we reveal rapid Ca^{2+} waves whose range defines which microglia will move to the damage site. Preventing their formation by chelating extracellular calcium is sufficient to suppress microglial targeting to damage sites, whereas local induction of Ca^{2+} signaling by photo-uncaging of IP3 attracts microglia in the absence of neuronal injury. Surprisingly, while we confirm that calcium-transmitted microglial attraction to damage requires ATP, we show that Ca^{2+} waves do not depend on ATP-signaling or on GAP junctions. Finally, we show that, via the activation of NMDA receptors, glutamate acts as a potent inducer of Ca^{2+}-wave-mediated microglial attraction.

RESULTS

Systematic Ablation of Neurons and Microglial Responses to Injury

We have previously described that the optically transparent embryonic zebrafish brain is patrolled by few (around 20) microglia, (Figures 1A–1C; (Peri and Nüsslein-Volhard, 2008)). We have used this system to study the response of an entire microglial cellular network to brain damage. We began our analysis by

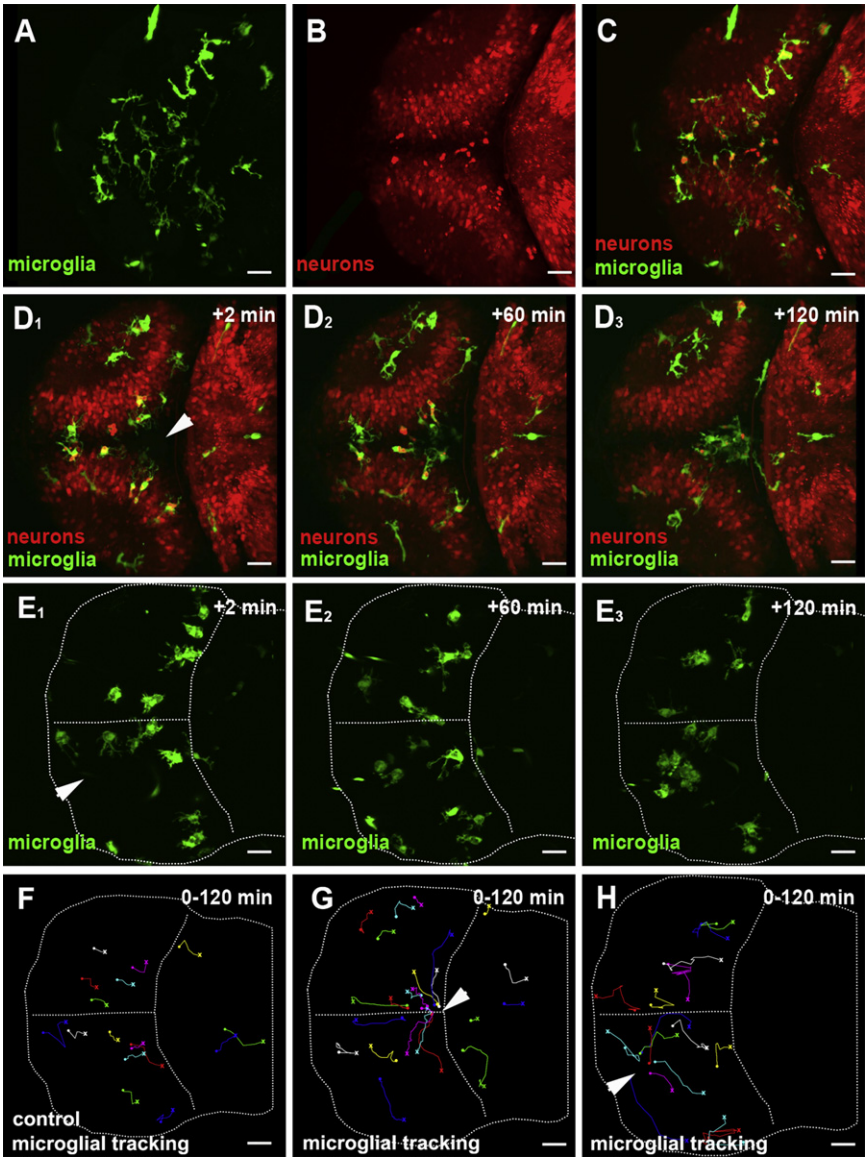

Figure 1. Microglial Migration upon Laser-Induced Neuronal Injuries

(A) Dorsal view of a 3 dpf larval brain. Microglia (pU1::Gal4-UAS-GFP).

(B) Dorsal view of a 3 dpf larval brain. Neurons (NBT::DsRed).

(C) Overlay of (A) and (B).

(D_1–D_3) Confocal time-lapse showing microglia (green) responding to a central injury (recording times indicated) (Movie S1, left). The injury site is marked with a white arrowhead.

(E_1–E_3) Confocal time-lapse showing microglia (green) responding to a single-hemisphere injury (recording times indicated) (Movie S1, right). The injury site is marked with a white arrowhead.

(F) Microglial cell tracking over 120 min in the preinjured brain. The starting point of individual tracks is marked with an X and the end point with a dot.

(G) Microglial cell tracking over 120 min upon central injury. The injury site is marked with a white arrowhead.

(H) Microglial cell tracking over 120 min upon single-hemisphere injury. The injury site is marked with a white arrowhead.

Scale bars for all images: 20 μm. All images were produced using an Olympus FV 1000 with a 40×/NA 1.15 objective.

See also Figure S1 and Movie S1.

defining the behavior of microglia in the preperturbed state. Cell tracking reveals that zebrafish microglia, like their mouse counterparts, show little cell body displacement and are mainly characterized by the generation of cellular branches that undergo rapid cycles of formation and withdrawal on a timescale of minutes (Figure 1F; Figures S2C and S2F available online) (Nimmerjahn et al., 2005; Peri and Nüsslein-Volhard, 2008). Next, we developed protocols for the systematic ablation of neurons using a diffraction-limited pulsed laser. We began by generating ablations in the center of the brain at an anatomical point between the two hemispheres that can be identified easily in all samples (Figures 1D_1–1D_3 and Figures S1A_1 and S1D). The ablation volume of 30 × 30 × 45 μm was confirmed both under the microscope and in histological sections and leads to the death of approximately 200 neurons without either damaging the blood-brain barrier or perturbing normal larval development (Figures S1A–S1D). Microglia coming from both brain hemispheres respond by accumulating at the site of the lesion (Figures 1D_1–1D_3 and 1G; Figures S2A and S2B; Movie S1, left) ($n = 20/20$; $p < 0.001$). This movement is characterized first by the formation of branches that can be as long as 50 μm pointing toward the ablation site (Figures 1D_2 and 2F_3; Movie S1), followed by the retraction of the cell rear at a speed of around 3.3 μm/min (Figures S2A and S2B; Movie S1). We next asked if changing the place of injury influences microglial responses. Indeed, comparable ablations located within one hemisphere only attract microglia from that same side of the brain, even though cells in the nonresponding side are as close to the wound site as responding cells (Figures 1E_1–1E_3 and 1H; Movie S1, right) ($n = 12/12$; $p < 0.001$). These experiments point to the existence of a long-range guidance system that might be unable to cross the brain midline.

Spatial and Temporal Correlation between Ca^{2+} Signaling and Microglial Responses

In search for the underlying guidance cue, we turned to Ca^{2+} signaling, as intercellular Ca^{2+} has been observed to increase upon mechanical stimulation of cultured cell lines (Charles et al., 1991). To monitor Ca^{2+} signaling in vivo we have generated a transgenic line where the GCaMP3.1 indicator (Tian et al., 2009) has been placed under the control of the ubiquitous beta-actin promoter. Importantly, ablations in the center of the brain generate a radial wave of Ca^{2+} elevation that travels

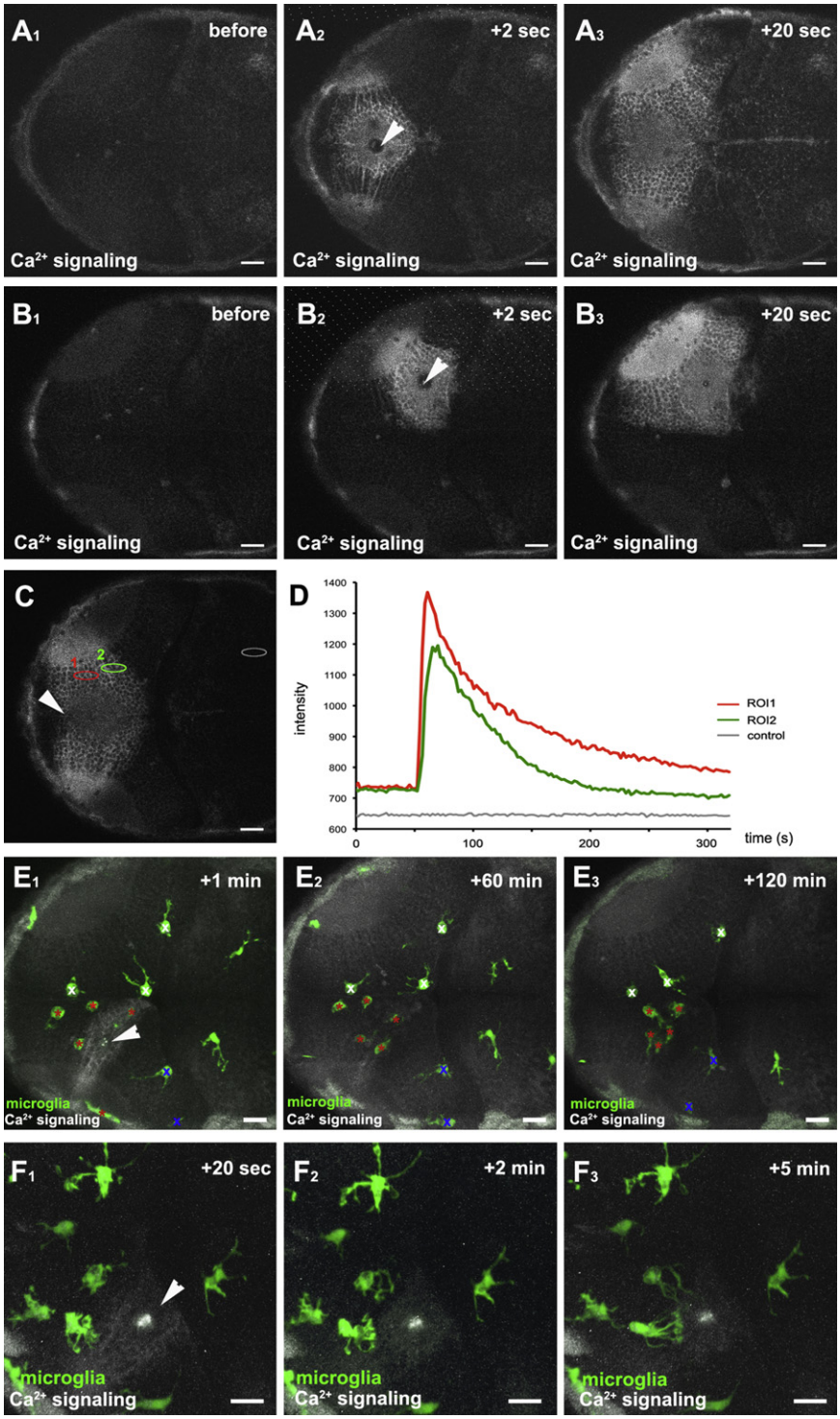

Figure 2. Neuronal Injuries Initiate Long-Range Ca^{2+} Transients in the Brain

(A_1–A_3) Dorsal views of a 3 dpf larval brain showing the time course of a Ca^{2+} wave (beta-actin::GCaMP3.1) forming upon central brain injury (Movie S2, upper left). The injury site is marked with a white arrowhead.

(B_1–B_3) Time course of a Ca^{2+} wave (beta-actin::GCaMP3.1) forming upon single-hemisphere injury (Movie S2, upper right). The injury site is marked with a white arrowhead.

(C) Ca^{2+} wave (beta-actin::GCaMP3.1) upon central brain injury with regions of interest (ROI1, ROI2, and control) for intensity measurements marked with red, green, and gray ellipses, respectively. The injury site is marked with a white arrowhead.

(D) Intensity plot of the Ca^{2+} signal over time measured in ROI1, ROI2, and control shown in (C).

(E_1–E_3) Time course of Ca^{2+}-wave (beta-actin::GCaMP3.1) and microglial movement (pU1::Gal4-UAS-TagRFP) upon killing of around 10 neurons (Movie S2, lower left). The injury site is marked with a white arrowhead. Microglial cells responding to the injury are marked with red asterisks, while microglia in the same hemisphere not responding to injury are labeled with blue Xs. Microglia in the other hemisphere are labeled with a white X.

(F_1–F_3) Time course of Ca^{2+} wave (beta-actin::GCaMP3.1) and microglial branching (pU1::Gal4-UAS-TagRFP) upon killing of around 10 neurons (Movie S2, lower right). The injury site is marked with a white arrowhead.

Scale bars for all images: 20 μm. All images were produced using an Olympus FV 1000 with a 40X/NA1.15 objective.

See also Movie S2.

across the brain at a speed of approximately 14 μm/s (Figures 2A_1–2A_3; Movie S2, upper left) ($n = 35/35$; $p < 0.001$). On the other hand, asymmetric injuries cause unilateral Ca^{2+} signaling that is confined to one side of the brain, stopping right at the midline (Figure 2B_1–2B_3; Movie S2, upper right) ($n = 22/22$; $p < 0.001$). Fluorescence intensity measurements show that waves are graded; cells closer to an injury site experience higher Ca^{2+} levels than distant cells, and these differences are maintained over time (Figures 2C and 2D). To learn more about the spatial correlation existing between Ca^{2+} signaling and microglial movement we created a smaller ablation volume encompassing approximately 10 cells. Remarkably, killing fewer cells generates shorter-range waves and only microglial cells that are close to the area marked by increased GCaMP3.1 activation branch and move toward the lesion (Figures 2E_1–2E_3; Movie S2, lower left) ($n = 14/14$; $p < 0.001$). Thus, the calcium wave scales with damage size, as does the number of microglial cells responding to damage, indicating a strong spatial correlation between these two events. Moreover, microglial cells polarize their branches within a minute upon exposure to high Ca^{2+} levels, indicating a strong temporal correlation between Ca^{2+} signaling and microglial responses (Figures 2F_1–2F_3; Movie S2, lower right) ($n = 8/8$; $p < 0.005$).

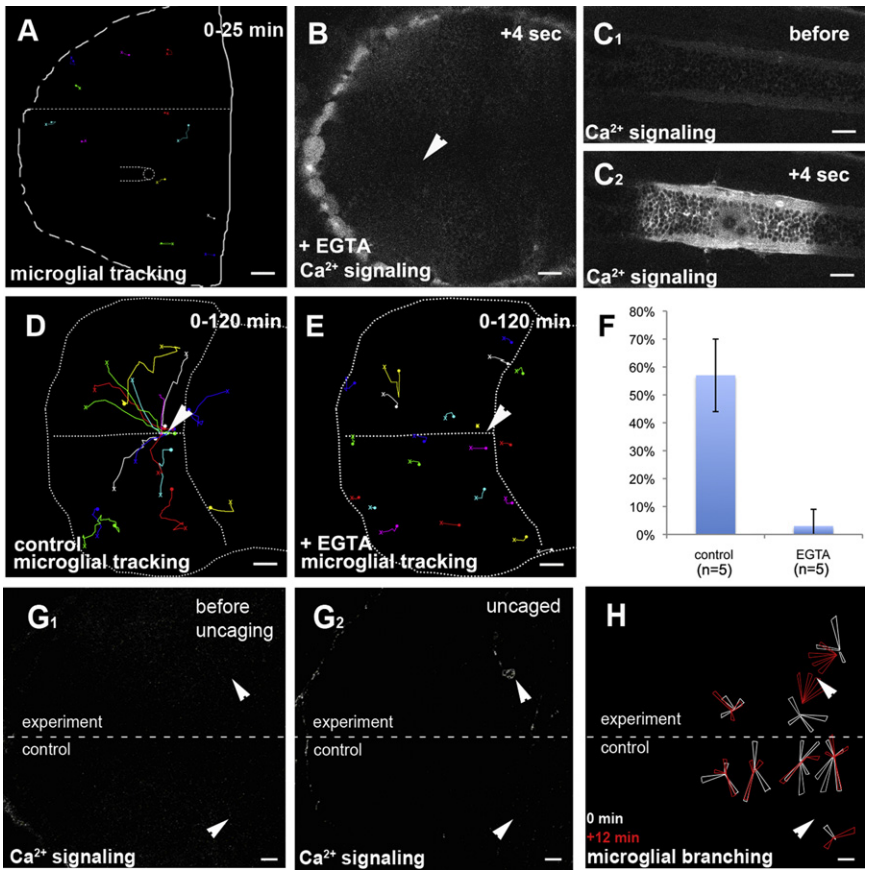

Figure 3. Ca^{2+} Signaling Prefigures and Guides Microglial Migration

(A) Microglial tracking (pU1::Gal4-UAS-TagRFP) upon control injection of water in a 3 dpf larval brain. The starting point of individual tracks is marked with an X and the end point with a dot.

(B) Injection of EGTA blocks the formation of Ca^{2+} waves (beta-actin::GCAMP3.1) upon laser injury (Movie S3, middle). The site of injury is marked with a white arrowhead.

(C_1 and C_2) Control injury in the trunk of the same embryo as in (B). Ca^{2+} imaging (beta-actin::GCAMP3.1) before (C_1) and after (C_2) injury (Movie S3, right).

(D) Cell tracking of microglia (pU1::Gal4-UAS-TagRFP) upon central brain injury in a control embryo. The white arrowhead marks the site of injury. The starting point of individual tracks is marked with an X and the end point with a dot.

(E) Cell tracking of microglia (pU1::Gal4-UAS-TagRFP) upon central brain injury in a EGTA injected embryo. The site of injury is marked with a white arrowhead. The starting point of individual tracks is marked with an X and the end point with a dot.

(F) Quantification of microglia movement to an injury site (percentage of microglia in the optic tectum responding to injury) in control (left, n = 5) and EGTA-injected brains (right, n = 5). Error bars represent standard deviations.

(G) Single-hemisphere injections of caged IP3 (experiment). Single-neuron uncaging leads to Ca^{2+} signaling (beta-actin::GCaMP3.1) in the injected, but not in the control, side. Laser uncaging sites before (G_1) and after (G_2) uncaging are marked by white arrowheads.

(H) Rose plot of microglial response to IP3 uncaging, showing microglia positions before (white) and 12 min after (red) uncaging.

Scale bars for all images: 20 μm. Images in (B)–(F) were produced using an Olympus FV 1000 with a 40×/NA1.15 objective. Images in (A) and (G)–(H) were done using an Andor Spinning Disk Confocal with a 20×/NA0.7 objective.

See also Figure S1 and Movies S3, S4, and S6.

Ca^{2+} Waves Are Necessary and Sufficient to Guide Microglia

To further investigate the requirement of Ca^{2+} signaling we have taken a pharmacological approach. First, we have established that control buffer injections under the microscope lead neither to Ca^{2+} wave formation nor to microglial movement (Figure 3A; Movie S3, left) ($n = 5/5$; $p < 0.05$). We injected non-membrane-permeable EGTA to chelate extracellular Ca^{2+}. As shown in Figure 3, EGTA injections prevented Ca^{2+} wave formation upon neuronal injury (Figure 3B; Movie S3, middle) ($n = 21/21$; $p < 0.001$). However, simultaneous laser injury in the spinal cord of the same embryo resulted in a robust Ca^{2+} wave, confirming that the EGTA effect is local (Figure $3C_1$ and $3C_2$; Movie S3, right). Most important, extracellular Ca^{2+} chelation, which has no effect on normal baseline microglial cell motility, quantified in terms of branch extension and retraction speed, as in Nimmerjahn et al. (2005) (Figures S2C, S2D, and S2F; Movie S4, right), suppressed the targeting of microglia to the wound site, demonstrating the requirement for Ca^{2+} waves in this process (Figures 3D–3F; Figures S2A, and S2B; Movie S4, left) ($n = 5/5$; $p < 0.005$). Neither Thapsigargin ($n = 9/9$; $p < 0.005$), an intracellular Ca^{2+} modulator, nor carbenoxolone (CBX) ($n = 19/19$; $p < 0.001$) and flufenamic acid (FFA) ($n = 8/8$; $p < 0.005$), GAP junction inhibitors, had any effect on the Ca^{2+} wave propagation, suggesting that the observed processes do not depend on intracellular Ca^{2+} pools or GAP junctions, respectively (Figures $S1E_1$, $S1E_2$, $S1L_1$, and $S1L_2$; data not shown). We next determined whether Ca^{2+} signaling alone could attract microglial branching and movement in the absence of injury by local flash-uncaging of IP3 (Ellis-Davies, 2007). IP3 was injected specifically into one brain hemisphere, allowing the other to be used as an internal control (Figures $3G_1$ and $3G_2$; see also Figures $5A_1$ and $5A_2$ showing injection into one single hemisphere) ($n = 25/25$; $p < 0.001$). Upon uncaging of IP3, surrounding microglia respond by branching directly toward the uncaged spot (Figure 3H and Figures 5B–5D; Movie S6) ($n = 8/9$; $p < 0.05$). We tuned the uncaging protocol so that applying the same laser intensity to the uninjected-control hemisphere does not elevate Ca^{2+} levels, nor does it have an effect on surrounding microglial dynamics, indicating that the procedure is by itself not harmful to the tissue (Figures $3G_1$, $3G_2$, and 3H). We conclude that locally increased Ca^{2+} alone is sufficient to mimic microglial injury response and that Ca^{2+} signaling plays a key instructive role in the long-range propagation of injury signaling across the brain.

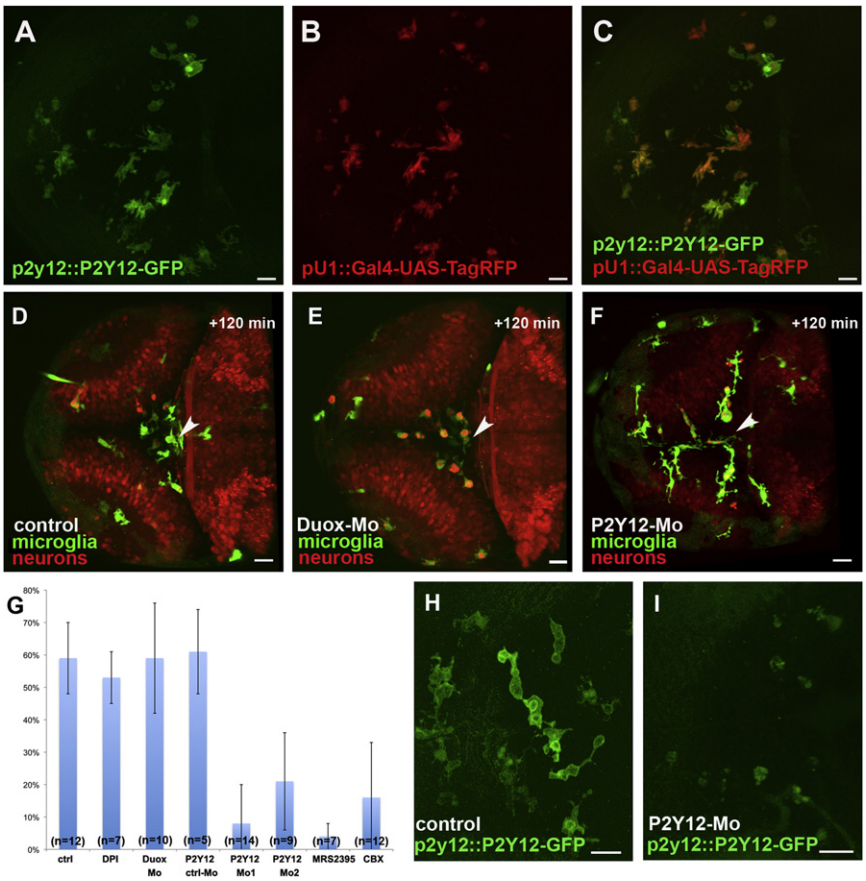

Figure 4. Microglial Movement Is Controlled via P2Y12 Activation

(A) Microglial cells express a P2Y12-GFP fusion protein under the endogenous P2Y12 promoter (p2y12::P2Y12-GFP).

(B) Microglia (pU1::Gal4-UAS-TagRFP).

(C) Overlay of (A) and (B).

(D–F) microglia (pU1::Gal4-UAS-GFP) and neurons (NBT::DsRed) in wild-type (D), Duox-morpholino-injected (E), and P2Y12-morpholino-injected embryos (F) 120 min after central injury. The sites of injury are marked with white arrowheads.

(G) Percentage of microglia in the optic tectum moving to the injury site in control (n = 12), DPI-treated (n = 7), Duox morphant (n = 10), MRS2395-treated (n = 7), CBX-treated (n = 12), P2Y12-Mo1-injected (n = 14), P2Y12 Mo2-injected (n = 9), and P2Y12 ctrl Mo-injected (n = 5) brains. Error bars represent standard deviations.

(H and I) Dorsal views of a 3 dpf larval brain, showing microglia in the p2y12::P2Y12-GFP line (H) and how P2Y12-morpholino injection strongly decreases P2Y12-GFP expression in these microglia (I).

Scale bars for all images: 20 μm. All images were produced using an Olympus FV 1000 with a 40×/NA1.15 objective.

See also Figure S2 and Movies S4 and S5.

Ca^{2+}-Stimulated Microglial Responses Require ATP, but Ca^{2+} Waves Are ATP Independent

We next turned our attention to the relationship between Ca^{2+} waves and the previously described response to neuronal injuries via activation of the microglial P2Y12 receptor by ATP (Haynes et al., 2006). To investigate the requirement for this receptor in our system, we generated a BAC transgenic line in which we fused GFP to the P2Y12 receptor via homologous recombination in bacteria. We found that, as in mouse, this receptor is expressed specifically in microglia (Figures 4A–4C) and P2Y12 knockdown experiments using two different ATG morpholinos severely affect GFP expression in the BAC transgenic embryos (Figures 4H and 4I). Both receptor knockdowns and pharmacological inhibition, using MRS2395, give the same phenotype and lead to a complete block of microglial responses to injury (Figures 4D, 4F, and 4G; Figures S2A and S2B). This is a specific phenotype, as P2Y12 morphant cells display the same baseline motility as wild-type microglia, quantified in terms of speed of branch extension and retraction (Figure S2C–S2F; Movie S4, right). Moreover, we also performed a functional assay and found that morphant microglia, which do not respond to injury, not only engulf apoptotic neurons but also actively move toward fluorescently labeled bacteria, collecting them with the same efficiency as wild-type microglia (Figures S1F, S1G, $S1I_1$–$S1I_3$, and S1J; Movie S5). To further test the role of ATP signaling in microglial migration toward neuronal injuries, we have taken several approaches. We have performed injections of apyrase (n = 7/7; $p < 0.01$), an ATP-hydrolyzing enzyme, masked the native ATP signaling by injecting large amounts of ATP into the brain, and knocked down P2Y12, the ATP receptor present on microglia. All approaches impair microglial-targeted migration toward neuronal injuries (Figures 4F, 4G, and 5L; Figures S2A and S2B; data not shown). Surprisingly, however, ATP injection did not induce a Ca^{2+} wave (Figure $5A_1$) (n = 22/22; $p < 0.001$) and ATP saturation (n = 12/12; $p < 0.001$), apyrase injection (n = 12/12; $p < 0.001$), and P2Y12 knockdown (n = 16/16; $p < 0.001$) had no influence on wave formation and propagation upon laser ablations in the brain (Figures $5A_2$ and 5K; Figures $S1H_1$ and $S1H_2$). Moreover, we found that while Ca^{2+} waves are ATP independent, Ca^{2+}-stimulated microglial responses require ATP, as microglial targeted movement induced by IP3 uncaging can be blocked by coinjecting apyrase into the brain (Figures 5E–5G; Movie S7, upper) (n = 8/9; $p < 0.05$) and by knocking down the P2Y12 receptor present on these cells (Figures 5H–5J; Movie S7, lower) (n = 7/8; $p < 0.05$). We speculate that high Ca^{2+} levels in neurons could lead to the release of ATP into the extracellular space, as shown in vitro (Liu et al., 2011). To test this, we have incubated transgenic embryos with CBX, a well-known ATP-release blocker that works at the level of Pannexin channels (Chekeni et al., 2010). This treatment blocks microglial targeted migration toward the wound without affecting Ca^{2+} wave formation (Figure 4G; Figures $S1L_1$, $S1L_2$, $S1M_1$, and $S1M_2$) (n = 12/12; $p < 0.001$). We conclude that Ca^{2+} signaling and microglial movement are likely to be coupled via ATP working in the extracellular space as chemoattractant. Consistent with this, diffusion of ATP from the tip of a needle

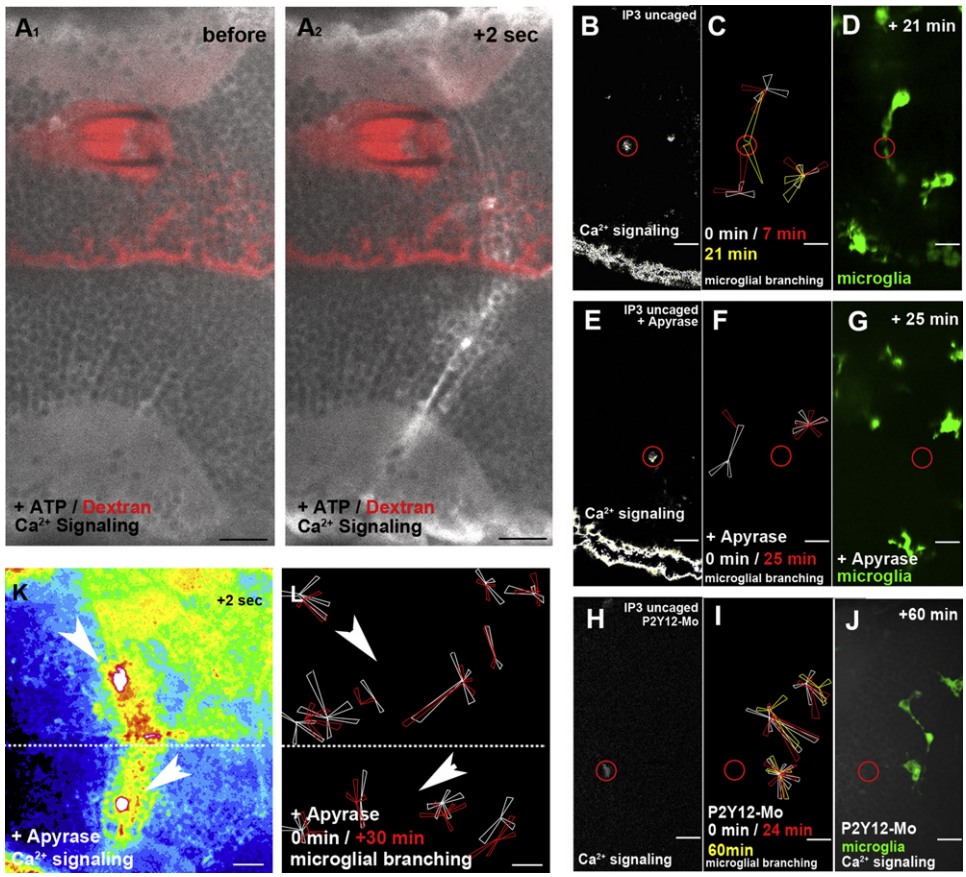

Figure 5. ATP Does Not Influence Ca^{2+} Wave Formation but Promotes Microglial Movement

(A_1) Injection of ATP does not promote Ca^{2+} wave formation (beta-actin::GCaMP3.1).

(A_2) Same ATP-injected embryo as in (A_1) shows normal Ca^{2+} wave formation upon laser injury.

(B) Ca^{2+} signaling (beta-actin::GCAMP3.1) after IP3 uncaging (Movie S6, left). The location of the uncaging is marked with a red circle.

(C) Rose plot of microglial response to IP3 uncaging showing images before uncaging (white) and 7 min (red) and 21 min (yellow) after uncaging.

(D) Microglial response (pU1::Gal4-UAS-TagRFP) in the same embryo as in (C) 21 min after IP3 uncaging (Movie S6, right).

(E) Ca^{2+} signaling (beta-actin::GCAMP3.1) upon IP3 uncaging in an embryo additionally injected with apyrase (Movie S7, upper left).

(F) Rose plot of microglial response to IP3 uncaging in an apyrase-injected brain showing images before (white) and 25 min after (red) uncaging.

(G) Microglial response (pU1::Gal4-UAS-TagRFP) in the same embryo as in (F) 25 min after IP3 uncaging (Movie S7, upper right).

(H) Ca^{2+} signaling (beta-actin::GCAMP3.1) upon IP3 uncaging in an embryo injected with P2Y12-Mo (Movie S7, lower left).

(I) Rose plot of microglial response to IP3 uncaging in a P2Y12-depleted brain showing microglia positions before (white) and 24 min (red) and 60 min (yellow) after uncaging.

(J) Microglial response (pU1::Gal4-UAS-TagRFP) in the same embryo as in (I) 60 min after IP3 uncaging (Movie S7, lower right).

(K) Ca^{2+} signaling (beta-actin::GCaMP3.1) upon laser injuries (white arrowheads) in an embryo injected with apyrase.

(L) Rose plot of microglial response to laser injury in the apyrase-injected embryo as in (K), showing microglia positions before (white) and 30 min after (red) injury.

Scale bars for all images: 20 μm. All images were produced using an Andor Spinning Disk Confocal with a 20×/NA0.7 objective.

See also Movies S6, S7, and S8.

attracts surrounding microglia toward the injury at an average speed of 0.0625 μm/s (Figures S2G_1–S2H; Movie S8) (n = 12/12; $p < 0.001$).

As it has been shown that zebrafish leukocytes are attracted toward a wound in the caudal fin via the formation of an H_2O_2 gradient (Niethammer et al., 2009), we tested for the requirement of H_2O_2 signaling in microglial migration to brain lesions. While we could confirm what has been reported for wounding of the fin, we found that knockdown morpholino injections (n = 10/10; $p < 0.001$) and treatment with DPI (n = 7/7; $p < 0.01$), an inhibitor of the H_2O_2-producing enzyme DUOX have no effect on microglial recruitment to brain lesions, indicating that in vertebrates, different systems are in place to guide immune cells to wounds (Figures 4E and 4G; Figures S1K, S2A, and S2B).

Glutamate Evokes Ca^{2+} Waves and Microglial Migration via NMDA-Receptor Activation

We have shown that intercellular Ca^{2+} waves guide microglia toward brain injuries in an ATP-dependent manner. However, as Ca^{2+} waves are ATP independent, it remained to be established what could promote their formation and propagation. By injecting directly into the brain, we have ruled out a role for

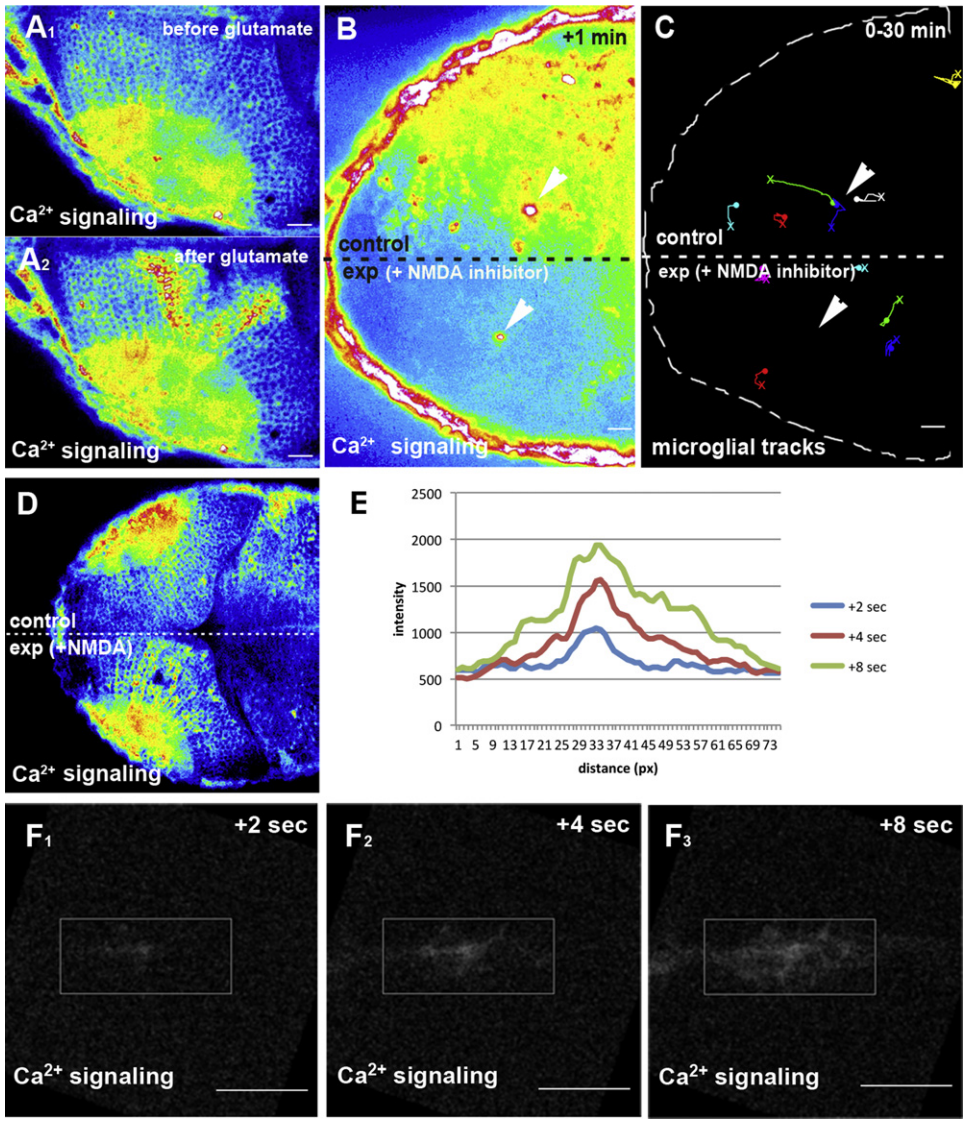

Figure 6. Glutamate Promotes Ca^{2+} Signaling and Microglial Movement

(A) Ca^{2+} signaling (beta-actin::GCAMP3.1) before (A_1) and after (A_2) injection of glutamate.

(B) Single-lobe injection (exp) of NMDA inhibitors blocks Ca^{2+}-wave (beta-actin::GCAMP3.1) formation upon laser injury. Laser ablation sites are marked by white arrowheads.

(C) Microglial tracking in the same NMDA-inhibitor-injected embryo as in (B). Laser ablation sites are marked by white arrowheads. The starting point of individual tracks is marked with an X and the end point with a dot.

(D) Single-lobe injection (exp) of NMDA induces Ca^{2+}-wave (beta-actin::GCAMP3.1) formation.

(E) Intensity plot of the Ca^{2+} signal upon NMDA uncaging measured 2 s, 4 s, and 8 s after uncaging within the ROI shown in (F).

(F) Ca^{2+} signaling (beta-actin::GCAMP3.1) 2 s (F_1), 4 s (F_2), and 8 s (F_3) after uncaging of NMDA (Movie S11, upper left).

Scale bars for all images: 20 μm. All images were produced using an Andor Spinning Disk Confocal with a 20×/NA0.7 objective.

See also Movies S9, S10, and S11.

ADP and UTP in the process and found that, on the contrary, glutamate evokes intracellular Ca^{2+} elevation in the surrounding tissue, as observed in laser injury experiments (Figures $6A_1$ and $6A_2$; Movie S9) ($n = 6/6$; $p < 0.05$).

Interestingly, this glutamate-induced Ca^{2+} elevation propagates only upon continuous injection, indicating that glutamate cannot be considered a simple trigger of a runaway self-sustained process (Movie S9). To elucidate whether glutamate is indeed involved in Ca^{2+} signaling and microglial migration downstream of laser-induced injuries, we turned to the glutamate receptors and took advantage of the large collection of inhibitors and agonists. Indeed, we found that injection of NMDA-receptor inhibitors, but not of AMPA inhibitors, in one brain hemisphere blocks laser-induced Ca^{2+} wave formation in the experiment side, while waves are still visible in the uninjected control side (Figure 6B; Movie S10; data not shown) ($n = 18/20$;

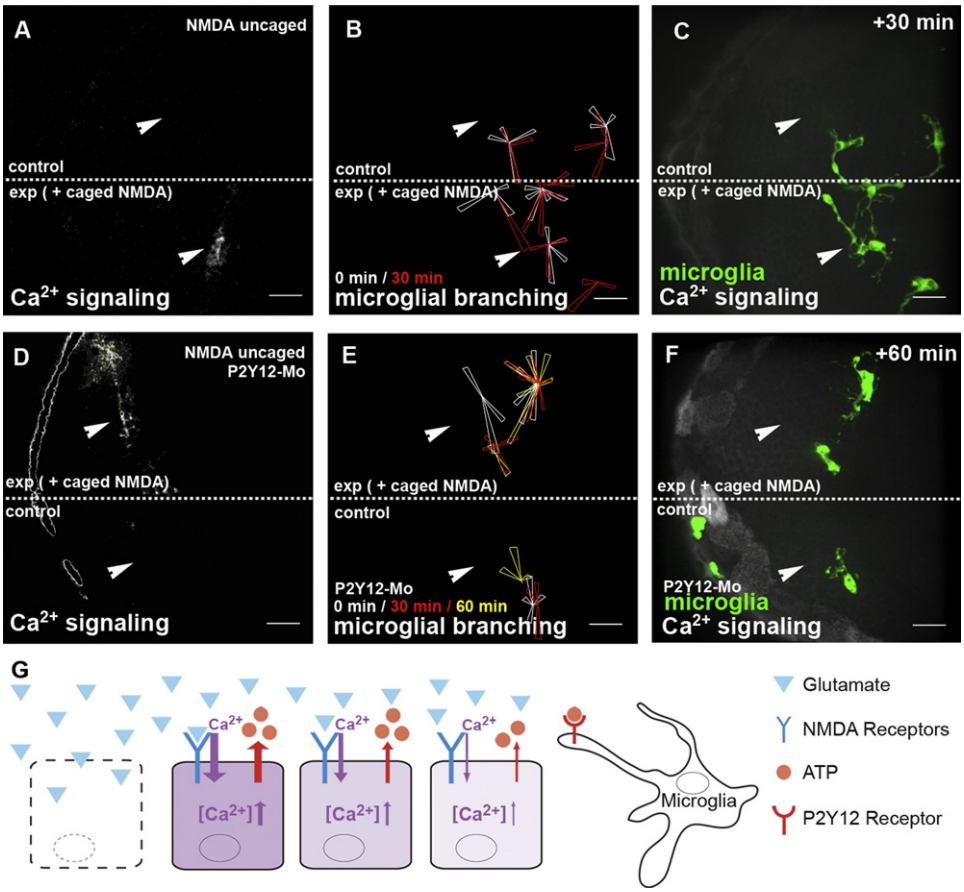

Figure 7. Microglial Branching toward Sites of Glutamate Signaling Is Mediated via the Microglial ATP Receptor P2Y12

(A) Single-hemisphere injections of caged NMDA. Uncaging leads to Ca^{2+} signaling (beta-actin::GCaMP3.1) in the injected, but not in the control, side (Movie S11, upper). Laser uncaging sites are marked by white arrowheads.

(B) Rose plot of microglial response to NMDA uncaging, showing microglia positions before (white) and 30 min after (red) uncaging.

(C) Microglial response (pU1::Gal4-UAS-TagRFP) in the same embryo as in (B) 30 min after NMDA uncaging (Movie S11, upper).

(D) Single-hemisphere injections of caged NMDA in P2Y12-Mo-injected embryos. Laser uncaging sites are marked by white arrowheads.

(E) Rose plot of microglial response to NMDA uncaging in P2Y12-depleted brains showing microglia positions before (white) and 30 min (red) and 60 min (yellow) after uncaging.

(F) Microglial response (pU1::Gal4-UAS-TagRFP) in the same embryo as in (E) 60 min after NMDA uncaging (Movie S11, lower).

(G) Schematic overview of the microglial response to injury. Glutamate leads to an influx of Ca^{2+}, which in turn leads to release of ATP that is sensed by microglia via their P2Y12 receptor.

Scale bars for all images: 20 μm. All images were produced using an Andor Spinning Disk Confocal with a 40x/NA1.15 objective.

See also Movie S11.

$p < 0.001$). Interestingly, in the same embryos, microglial responses to laser damage occur only in the uninjected control side, while cells in the NMDA-inhibitor-injected hemisphere fail to respond to injury (Figure 6C) ($n = 8/8$; $p < 0.01$). In line with this, the injection of NMDA, a well-known agonist of the NMDA receptors, also promotes Ca^{2+} elevation (Figure 6D) ($n = 24/24$; $p < 0.001$). To further test this, we performed local flash-uncaging of caged NMDA and found that this promotes the development of a graded Ca^{2+} wave (Figures 6E and $6F_1$–$6F_3$; Movie S11, upper left) ($n = 25/25$; $p < 0.001$). Nearby microglia respond by branching toward the wave (Figures 7A–7C; Movie S11, upper right) ($n = 14/15$; $p < 0.001$). As for the IP3 uncaging experiments, caged NMDA was injected specifically into one brain hemisphere, using the other as an internal control (Figures 7A–7C; see also Figures $5A_1$ and $5A_2$, which show injections into a single hemisphere). Again, we optimized the uncaging protocol such that the same laser intensity applied to the uninjected-control hemisphere does not elevate Ca^{2+} levels, nor does it have an effect on surrounding microglial dynamics, indicating that the procedure is by itself not harmful for the tissue (Figures 7A–7C). Thus, we conclude that in the brain, neuronal injury evokes a Ca^{2+} wave and microglial migration via activation of NMDA receptors. As NMDA receptors are known Ca^{2+}-channels, their involvement in this process is consistent with our previous finding that only extracellular Ca^{2+} modulators, such as EGTA, block Ca^{2+} wave formation and microglial movement upon injury (Figure 3B). To exclude that NMDA might act on microglia directly by stimulating their migration, we uncaged NMDA

in P2Y12 morphant brains. Upon uncaging, morphant cells fail to branch toward the source of NMDA uncaging (Figures 7D–7F; Movie S11, lower right) (n = 10/12; $p < 0.05$), indicating that NMDA stimulates microglia by providing ATP via a mechanism that proceeds across the brain in the form of a Ca^{2+} wave (Figure 7G). These graded intercellular Ca^{2+} levels are most likely required to maintain the ATP guiding cue that is responsible for transmitting positional information to the P2Y12-expressing microglia.

DISCUSSION

Long-Range Ca^{2+} Waves Transmit Death Signals across the Brain

Here, we present a system that allows the response of the entire microglial network to neuronal injury to be studied in a living brain. Targeted laser neuronal ablations in brains of transgenic calcium reporter fish show that rapid Ca^{2+} waves determine which microglia will move to the damage site. Indeed, preventing Ca^{2+} waves suppresses microglial migration, whereas local induction of Ca^{2+} signaling is sufficient to attract microglia in the absence of neuronal injury. Intercellular Ca^{2+} waves have long been known to occur in vitro (Charles et al., 1991), but their functional significance in vivo has been mostly unclear. Recently, Ca^{2+} reporters and in vivo imaging have been used to show that in adult mice, changes in astrocytic Ca^{2+} levels occur in response to neuronal stimulation, indicating that in the brain, Ca^{2+} signaling under physiological conditions mediates communication between neurons and glia (Wang et al., 2006). Here, we show that intercellular Ca^{2+} signaling is also used to mediate communication between glia, neurons, and a third player in the system, the microglia. Indeed, via these waves, microglia are guided toward dead neurons. These Ca^{2+} ramps depend directly on glutamate signaling and NMDA-receptor activation, and upon NMDA uncaging, we observe the formation of small and graded Ca^{2+} waves that start from a point source of NMDA signaling. In turn, Ca^{2+} signaling is responsible for providing ATP guidance to microglia. This guidance is likely to be graded, as saturation by injecting large amounts of ATP into the brain abolishes microglial-targeted migration (Davalos et al., 2005). As recent publications have suggested that microglia sense the neuronal functional state and respond by modulating synaptic activity, it is tempting to speculate that there might be a significant overlap in the molecular and cellular mechanisms that guide these cells toward dying and malfunctioning neurons (Wake et al., 2009; Zhong et al., 2010).

Molecular Mechanisms Involved in Long-Range Ca^{2+} Signaling

We have found that one function of glutamate-dependent Ca^{2+} waves is the establishment of an ATP guidance cue that is responsible for transmitting positional information across the brain to the P2Y12-expressing microglia. Contrary to what is generally hypothesized, we find that these Ca^{2+} waves are ATP independent, as we see no role for ATP in their formation and propagation. Indeed, in several in vitro studies, ATP has been shown to increase intracellular Ca^{2+} levels via activation of P2Y receptors that promote the exit of Ca^{2+} from endoplasmic reticulum stores (Fischer et al., 2009; Ryu et al., 2010; Butt, 2011). Moreover, adding EGTA to the medium of astrocytic cell cultures has no effect on glutamate-mediated Ca^{2+} signaling, indicating that Ca^{2+} is liberated from intracellular stores. It has been suggested that extracellular Ca^{2+} is only needed to sustain these intercellular Ca^{2+} waves (Cornell-Bell et al., 1990; Charles et al., 1991). Thus, our in vivo work shows that several mechanisms might be in place to promote and sustain intercellular Ca^{2+} waves. Moreover, it was also shown recently that microglia respond to glutamate directly in an ATP independent manner via the activation of AMPA receptors present on these cells (Liu et al., 2009). Here, however, we find that in the presence of neuronal injuries, glutamate promotes microglial migration in an ATP-dependent manner via NMDA-receptor activation and formation of Ca^{2+} waves that travel across the brain. Differences in the underlying molecular machineries are likely to reflect different cellular compositions and tissues, stressing the importance of investigating biological contexts in which cellular configuration, morphology, and dynamics are preserved.

Different Guidance Cues Are in Place in the Vertebrate System to Attract Leukocytes toward Tissue Injuries

The process by which complex spatial information, in the form of diffusible molecules, is interpreted by motile cells to elicit unequivocal cell behavior is a central topic in both cell and developmental biology. Leukocytes are an ideal vehicle for studying this problem, as they move rapidly in response to tissue injuries. Considering that these cells play a central role in the subsequent wound repair it is surprising how little we know about how they are attracted to the site of injury. The zebrafish larva has emerged as an ideal model system to study leukocyte cell migration (Traver et al., 2003; Trede et al., 2004). Using both reverse genetic approaches and live imaging of GFP-labeled leukocytes, Niethammer and colleagues have shown that upon manual injury of the larval fin fold, highly motile leukocytes migrate to the injury in response to a wave of reactive oxygen species that propagates from the site of damage throughout the surrounding epithelium (Niethammer et al., 2009). Interestingly, we could see no role for H_2O_2 signaling in our brain-wounding assays. The different nature of the inflicted damage, which is an open wound in the fin fold and an internal injury in the brain, might explain the different nature of the attractive cues. Indeed, several alert mechanisms could be in place to instruct leukocytes on the nature of the damage. Moreover, damaged cells themselves might differ in their competence to send out alert signals.

Finally, our discovery that long-range Ca^{2+} waves transmit damage signals across the brain offers a handle on understanding and controlling the collective behavior of the brain phagocytes. The demonstration that glutamate and Ca^{2+} are involved in this process provides great potential for future pharmacological modulation of microglial behavior.

EXPERIMENTAL PROCEDURES

Transgenic Fish Lines and Fish Maintenance

Fish were kept at 26.5°C in a 14 hr light/10 hr dark cycle. Embryos were collected by natural spawning and raised at 28.5°C in E3 solution. To avoid pigmentation, 0.003% PTU was added at 1 dpf. Staging of embryos was done according to Kimmel et al. (1995).

Microglia were visualized using pu1::Gal4-UAS-GFP and pu1::Gal4-UAS-TagRFP, and neurons were visualized using NBT-DsRed transgenic lines

(Peri and Nüsslein-Volhard, 2008). Blood vessels were visualized using fli1::GFP transgenic fish (Lawson and Weinstein, 2002). To monitor calcium levels in the brain, a stable transgenic line was generated expressing GCaMP3.1 (Tian et al., 2009) under the zebrafish beta-actin promotor (beta-actin::GCaMP3.1). To obtain transgenic fish, the beta-actin::GCaMP3.1 construct was flanked by *tol2* sites and injected into one-cell stage embryos together with *tol2*-transposase. Injected embryos were raised, and adult fish were screened for transgenic offspring. F1 and F2 fish were used for experiments. P2Y12 expression was shown by fusion of GFP to the C terminus of P2Y12 via BAC homologous recombination in bacteria (Yang et al., 2006; Suster et al., 2009). The modified BAC was injected into one-cell stage embryos. Injected embryos were raised, and adult fish were screened for transgenic offspring. F1 and F2 fish were used for experiments.

Confocal Imaging and Laser Injury

For live imaging, 3 dpf and 4 dpf zebrafish larvae were anesthetized in 0.01% tricaine and embedded in 1.5% low-melting-point agarose. Imaging was performed using the Olympus FV 1000 and the Andor Spinning Disk Confocal with 20×/NA 0.7 and 40×/NA 1.15 objectives. In general, for full brain recordings we captured 30–40 z-stacks spanning 45–60 μM of the fish brain. For Ca^{2+} imaging 1–10 z-stacks were captured, spanning up to 15 μM. Images were flattened by maximum projection in Imaris (Bitplane) and Fiji. Lesions were generated using a pulsed 532 nm laser coupled to the FV 1000 and a pulsed 355 nm laser coupled to the Andor Spinning Disk. Images were analyzed using both Imaris (Bitplane) and Fiji software. Numbers of samples per experiment, as well as p values, are indicated in the text. p values were calculated using a binomial probability function.

Genetic and Pharmacological Perturbations

Morpholino oligonucleotides (P2Y12: 5′-AGCTGCGTTGTTTGCTCCA TTGAT-3′; P2Y12-Mo2: CCTGCTGGGTGAAGTAATGAAGTCC; P2Y12-ctrl-Mo: AGC AGCCTTGTCTGCTGCATTCAT; Duox: 5′- AGTGAATTAGAGAAATGCACCTT TT-3′ (Niethammer et al., 2009) were obtained from Gene Tools. These were injected at a concentration of 0.3 mM with 0.2% Phenolred (Sigma) and 0.1 M KCl (Sigma) into one-cell stage zebrafish embryos. P2Y12 Morpholino knockdown was confirmed by injecting the P2Y12 morpholino into the p2Y12::P2Y12-GFP line (Figures 4H and 4I). RT-PCR was performed to test for the splicing effect of the Duox morpholino (Figure S1K). To interfere with calcium signaling and the microglial response, we used the following chemicals: EGTA (0.5 M) (Sigma), MRS2395 (45 μM) (Sigma), DPI (100 μM) (Sigma), Thapsigargin (150 μM) (Sigma), CBX (50 μM) (Sigma), FFA (1 μM) (Sigma), Alexa Fluor 647 ATP (5 mM) (Invitrogen), apyrase (90 u/ml) (Sigma), a mixture of D(−)-AP5 (5 mM) and MK-801 (3 mM) (both from Sigma), NPE-caged IP3 (800 μM) (Invitrogen), glutamate (9 mM) (Sigma), NMDA (9 mM) (Sigma), and MNI-caged NMDA (10 mM) (Tocris Bioscience). These were injected into the optic tectum of anesthetized larvae using a micromanipulator attached to the Andor Spinning Disk. Prior to injection, caged IP3 was mixed with pluronic F127 (final concentration 0.2%) (Invitrogen). Uncaging was achieved by flash photolysis of the caging group with UV illumination at 355 nm. In all uncaging experiments, we included controls to test whether similar stimulations triggered Ca^{2+} signaling in the neurons in the absence of the caged compounds. All injection solutions were mixed with Alexa Fluor 647 dextran (1:1000) (Invitrogen) prior to usage.

Bacterial Infections

E. coli (DH5α) carrying the dsRED-expressing pGEMDs3 plasmid (van der Sar et al., 2003) were grown in standard Luria Bertani medium containing ampicillin (50 μg/ml). For infections, a 3 ml overnight culture was centrifuged for 3 min at 4,000 g and the pellet washed with PBS. After washing, the pellet was resuspended in PBS. Bacteria were injected into the optic tectum of anesthetized larvae using a micromanipulator attached to the Andor Spinning Disk.

SUPPLEMENTAL INFORMATION

Supplemental Information includes two figures and eleven movies and can be found with this article online at doi:10.1016/j.devcel.2012.04.012.

ACKNOWLEDGMENTS

We would like to thank Gerrit Heuvelman and Lars Hufnagel for implementing the laser cutter and Ivo Telly for constructing the micromanipulator on the Andor Spinning Disk system. We are grateful to the Advanced Light Microscopy Facility (EMBL, Heidelberg) for assistance with microscope imaging. We would like to thank Olympus Europe for continuous support of the Advanced Light Microscopy Facility. We are grateful to Annette Schmidt for suggesting the use of GCaMP3.1 for Ca^{2+} imaging. Thanks to Sabine Fischer for producing brain sections. We thank Andreas Kunze and Darren Gilmour for providing critical reagents for the generation of the P2Y12 BAC line. Thanks to Darren Gilmour, Alexander Aulehla, Timm Schlegelmilch, Fargol Mazaheri, and Kerstin Richter for critical reading of this manuscript. D.S. was supported by an EMBO postdoctoral fellowship and C.M. by an ERC starting grant to F.P.

Received: October 10, 2011
Revised: February 21, 2012
Accepted: April 12, 2012
Published online: May 24, 2012

REFERENCES

Butt, A.M. (2011). ATP: a ubiquitous gliotransmitter integrating neuron-glial networks. Semin. Cell Dev. Biol. *22*, 205–213.

Charles, A.C., Merrill, J.E., Dirksen, E.R., and Sanderson, M.J. (1991). Intercellular signaling in glial cells: calcium waves and oscillations in response to mechanical stimulation and glutamate. Neuron *6*, 983–992.

Chekeni, F.B., Elliott, M.R., Sandilos, J.K., Walk, S.F., Kinchen, J.M., Lazarowski, E.R., Armstrong, A.J., Penuela, S., Laird, D.W., Salvesen, G.S., et al. (2010). Pannexin 1 channels mediate "find-me" signal release and membrane permeability during apoptosis. Nature *467*, 863–867.

Chen, S.-K., Tvrdik, P., Peden, E., Cho, S., Wu, S., Spangrude, G., and Capecchi, M.R. (2010). Hematopoietic origin of pathological grooming in Hoxb8 mutant mice. Cell *141*, 775–785.

Cornell-Bell, A.H., Finkbeiner, S.M., Cooper, M.S., and Smith, S.J. (1990). Glutamate induces calcium waves in cultured astrocytes: long-range glial signaling. Science *247*, 470–473.

Davalos, D., Grutzendler, J., Yang, G., Kim, J.V., Zuo, Y., Jung, S., Littman, D.R., Dustin, M.L., and Gan, W.-B. (2005). ATP mediates rapid microglial response to local brain injury in vivo. Nat. Neurosci. *8*, 752–758.

David, S., and Kroner, A. (2011). Repertoire of microglial and macrophage responses after spinal cord injury. Nat. Rev. Neurosci. *12*, 388–399.

Ellis-Davies, G.C.R. (2007). Caged compounds: photorelease technology for control of cellular chemistry and physiology. Nat. Methods *4*, 619–628.

Fischer, W., Appelt, K., Grohmann, M., Franke, H., Nörenberg, W., and Illes, P. (2009). Increase of intracellular Ca^{2+} by P2X and P2Y receptor-subtypes in cultured cortical astroglia of the rat. Neuroscience *160*, 767–783.

Hanisch, U.-K., and Kettenmann, H. (2007). Microglia: active sensor and versatile effector cells in the normal and pathologic brain. Nat. Neurosci. *10*, 1387–1394.

Haynes, S.E., Hollopeter, G., Yang, G., Kurpius, D., Dailey, M.E., Gan, W.-B., and Julius, D. (2006). The P2Y12 receptor regulates microglial activation by extracellular nucleotides. Nat. Neurosci. *9*, 1512–1519.

Kimmel, C.B., Ballard, W.W., Kimmel, S.R., Ullmann, B., and Schilling, T.F. (1995). Stages of embryonic development of the zebrafish. Dev. Dyn. *203*, 253–310.

Lawson, N.D., and Weinstein, B.M. (2002). In vivo imaging of embryonic vascular development using transgenic zebrafish. Dev. Biol. *248*, 307–318.

Liu, G.J., Nagarajah, R., Banati, R.B., and Bennett, M.R. (2009). Glutamate induces directed chemotaxis of microglia. Eur. J. Neurosci. *29*, 1108–1118.

Liu, T., Sun, L., Xiong, Y., Shang, S., Guo, N., Teng, S., Wang, Y., Liu, B., Wang, C., Wang, L., et al. (2011). Calcium triggers exocytosis from two types of organelles in a single astrocyte. J. Neurosci. *31*, 10593–10601.

Moreira, S., Stramer, B., Evans, I., Wood, W., and Martin, P. (2010). Prioritization of competing damage and developmental signals by migrating macrophages in the Drosophila embryo. Curr. Biol. *20*, 464–470.

Napoli, I., and Neumann, H. (2009). Microglial clearance function in health and disease. Neuroscience *158*, 1030–1038.

Neumann, H., Kotter, M.R., and Franklin, R.J.M. (2009). Debris clearance by microglia: an essential link between degeneration and regeneration. Brain *132*, 288–295.

Niethammer, P., Grabher, C., Look, A.T., and Mitchison, T.J. (2009). A tissue-scale gradient of hydrogen peroxide mediates rapid wound detection in zebrafish. Nature *459*, 996–999.

Nimmerjahn, A., Kirchhoff, F., and Helmchen, F. (2005). Resting microglial cells are highly dynamic surveillants of brain parenchyma in vivo. Science *308*, 1314–1318.

Pangrsic, T., Potokar, M., Stenovec, M., Kreft, M., Fabbretti, E., Nistri, A., Pryazhnikov, E., Khiroug, L., Giniatullin, R., and Zorec, R. (2007). Exocytotic release of ATP from cultured astrocytes. J. Biol. Chem. *282*, 28749–28758.

Paolicelli, R.C., Bolasco, G., Pagani, F., Maggi, L., Scianni, M., Panzanelli, P., Giustetto, M., Ferreira, T.A., Guiducci, E., Dumas, L., et al. (2011). Synaptic pruning by microglia is necessary for normal brain development. Science *333*, 1456–1458.

Peri, F., and Nüsslein-Volhard, C. (2008). Live imaging of neuronal degradation by microglia reveals a role for v0-ATPase a1 in phagosomal fusion in vivo. Cell *133*, 916–927.

Ransohoff, R.M., and Cardona, A.E. (2010). The myeloid cells of the central nervous system parenchyma. Nature *468*, 253–262.

Ryu, S.-Y., Peixoto, P.M., Won, J.H., Yule, D.I., and Kinnally, K.W. (2010). Extracellular ATP and P2Y2 receptors mediate intercellular Ca^{2+} waves induced by mechanical stimulation in submandibular gland cells: Role of mitochondrial regulation of store operated Ca^{2+} entry. Cell Calcium *47*, 65–76.

Schlegelmilch, T., Henke, K., and Peri, F. (2011). Microglia in the developing brain: from immunity to behaviour. Curr. Opin. Neurobiol. *21*, 5–10.

Striedinger, K., Meda, P., and Scemes, E. (2007). Exocytosis of ATP from astrocyte progenitors modulates spontaneous Ca^{2+} oscillations and cell migration. Glia *55*, 652–662.

Suster, M.L., Sumiyama, K., and Kawakami, K. (2009). Transposon-mediated BAC transgenesis in zebrafish and mice. BMC Genomics *10*, 477.

Tian, L., Hires, S.A., Mao, T., Huber, D., Chiappe, M.E., Chalasani, S.H., Petreanu, L., Akerboom, J., McKinney, S.A., Schreiter, E.R., et al. (2009). Imaging neural activity in worms, flies and mice with improved GCaMP calcium indicators. Nat. Methods *6*, 875–881.

Traver, D., Herbomel, P., Patton, E.E., Murphey, R.D., Yoder, J.A., Litman, G.W., Catic, A., Amemiya, C.T., Zon, L.I., and Trede, N.S. (2003). The zebrafish as a model organism to study development of the immune system. Adv. Immunol. *81*, 253–330.

Trede, N.S., Langenau, D.M., Traver, D., Look, A.T., and Zon, L.I. (2004). The use of zebrafish to understand immunity. Immunity *20*, 367–379.

van der Sar, A.M., Musters, R.J.P., van Eeden, F.J.M., Appelmelk, B.J., Vandenbroucke-Grauls, C.M.J.E., and Bitter, W. (2003). Zebrafish embryos as a model host for the real time analysis of Salmonella typhimurium infections. Cell. Microbiol. *5*, 601–611.

Wake, H., Moorhouse, A.J., Jinno, S., Kohsaka, S., and Nabekura, J. (2009). Resting microglia directly monitor the functional state of synapses in vivo and determine the fate of ischemic terminals. J. Neurosci. *29*, 3974–3980.

Wang, X., Lou, N., Xu, Q., Tian, G.-F., Peng, W.G., Han, X., Kang, J., Takano, T., and Nedergaard, M. (2006). Astrocytic Ca^{2+} signaling evoked by sensory stimulation in vivo. Nat. Neurosci. *9*, 816–823.

Wood, W., and Jacinto, A. (2007). Drosophila melanogaster embryonic haemocytes: masters of multitasking. Nat. Rev. Mol. Cell Biol. *8*, 542–551.

Yang, Z., Jiang, H., Chaichanasakul, T., Gong, S., Yang, X.W., Heintz, N., and Lin, S. (2006). Modified bacterial artificial chromosomes for zebrafish transgenesis. Methods *39*, 183–188.

Zhong, Y., Zhou, L.-J., Ren, W.-J., Xin, W.-J., Li, Y.-Y., Zhang, T., and Liu, X.-G. (2010). The direction of synaptic plasticity mediated by C-fibers in spinal dorsal horn is decided by Src-family kinases in microglia: the role of tumor necrosis factor-α. Brain Behav. Immun. *24*, 874–880.

Zimmermann, H. (2000). Extracellular metabolism of ATP and other nucleotides. Naunyn Schmiedebergs Arch. Pharmacol. *362*, 299–309.